Carbonates Evaporites (2013) 28:89–94
DOI 10.1007/s13146-013-0143-8

ORIGINAL ARTICLE

Analysis of hydrogeological parameters and numerical modeling groundwater in a karst watershed, southwest China

Xi Chen · Yanfang Zhang · Yanyu Zhou · Zhicai Zhang

Accepted: 2 February 2013 / Published online: 12 March 2013

Abstract A numerical groundwater model was developed on the basis of a conceptualized, equivalent, continuous medium for a karst basin located in Guizhou Province, southwest China. In this model, simulation of underground drainage and groundwater–river interactions were executed using the Drain and River packages of MODFLOW, respectively. Hydraulic conductivities were first determined using flow recession analysis methods proposed by Brutsaert and Lopez (Water Resour Res 34(2):233–240, 1998) and Mendoza et al. (J Hydrol 279: 57–69, 2003). These parameters, together with recharge from precipitation, were further calibrated against observed water levels of subterranean rivers during 1988 and 1989 at three observation stations. The established model can be used to simulate temporal and spatial variations of groundwater levels and subterranean river discharges. The simulated results demonstrate that the total aquifer recharge comes mostly from precipitation and river leakage. Precipitation recharge and river leakage are about 70 and 13 % of the total aquifer recharge, respectively. Meanwhile, most discharge of the study watershed is from subterranean rivers. It accounts for 62 % of the total discharge and river drains only 8 % of the total discharge.

Keywords Hydrogeological parameters · Numerical modeling groundwater · Karst watershed · Southwest China

X. Chen (✉) · Y. Zhang · Y. Zhou · Z. Zhang
State Key Laboratory of Hydrology-Water Resources and Hydraulic Engineering, Hohai University, Nanjing 210098, China
e-mail: xichen@hhu.edu.cn

Introduction

One of the largest, continuous karst areas in the world is located in Yunnan-Guizhou Plateau of southwest China. It has a population of 100 million. Carbonate rocks occupy an area of 730,600 km^2, about 41 % of the total area, among which the thick carbonate rocks is 540,800 km^2, about 31 % of the total area, and the thin carbonate rock interbeds 189,800 km^2, about 11 % of the total area (Lu 2007). In the karst region of southwest China, soils, developed on carbonate rocks, are generally 30–50 cm thick. Limestone fragments are mixed in soils and can act as a controlling factor for erosional rates and patterns in the landscape. Precipitation is typically 1,000–2,200 mm/year; average annual temperatures are mostly 16–22 °C, so climatic conditions are favorable for karst development. In developed karst areas with primarily soluble carbonate rocks, surface flows that run into a swallet or sinkhole may pass directly into a conduit or an underground river. Therefore, surface water is limited and groundwater is the primary water resource for domestic, agricultural, and industrial utilization.

Simulation of groundwater processes (hydraulic heads, groundwater fluxes, and spring discharges) is usually based on numerical groundwater models for describing porous Darcy flow in a single continuum media, for example, as in the MODFLOW and FEFLOW packages. They could be improved as a double continuum model for representing the flow conditions in the saturated zone of karst aquifers with an underground conduit-and-fracture network through a porous matrix, like MODFLOW-DCM (Sun et al. 2005). However, simulating these heterogeneous systems requires large amounts of data for a variety of properties, including the flow geometry and flow medium porosity, permeability, and transmissivity. For simplifying catchment properties

and meeting the objective of modeling general flow processes, some researchers attempt to model the aquifers as Darcian systems (Scanlon et al. 2003) and approach conduits as high permeability regions (Teutsch 1993; Wicks and Herman 1995; Eisenlohr et al. 1997). Others regard conduits as simple drains that do not alter the hydrograph response of an aquifer (Milanovic 1996; Torbarov 1976).

In the karst basin of southwest China, the drainage system usually consists of surface rivers and underground rivers. Groundwater is fed by precipitation and surface streamflow. Surface rivers mostly dry out in the drought season, and underground rivers become a primary drainage passage. Additionally, anisotropy resulting from fractured rocks dominates flow direction and concentration. Until now, few workers have attempted the quantitative modeling of this kind of system with strong anisotropy of fractured medium and surface rivers and underground rivers. The goal of this study is to use a physically based numerical model to simulate the flow processes in the fractured medium and exchanges between the groundwater flow and surface and underground rivers. The established model will be applied for estimating recharge and discharge of the karst aquifer.

Study area and site description

The study area, the Houzhai subterranean drainage in Puding County, Guizhou Province in southwestern China, with an area of 81 km^2, has typical cone karst and cockpit karst landforms (Fig. 1). The elevation of the study area varies from 1,200 to 1,550 m above the sea level, higher in the east and lower in the west. The cone peaks of the Houzhai watershed are generally 200–300 m above the adjacent doline depressions, and the cone surface relief and slopes are much steeper.

The study site has a subtropical wet monsoon climate. The mean annual temperature is 20.1 °C. The highest average monthly temperature is in July, and the lowest is in January. Annual precipitation is 920 mm, with a distinct summer wet season and a winter dry season. Average monthly humidity ranges from 74 to 78 %.

The main rock type in the study area is limestone that belongs to the Guanling group (T_2g) of the middle Triassic Period (Wang et al. 2002). Various carbonates formed in the middle of the Triassic Period are spread throughout the study area. The karst topography includes many bare funnels and sinkholes and a well-developed subterranean river network. Buried karst is located in the valleys and poljes, which are surrounded by karst mountain peaks.

The Houzhai subterranean drainage system consists of three main surface rivers, the Dengzhan, Haoying and Houzhai rivers, and a main subterranean river, the Dayouzhai (DYZ)-Maoshuikeng (MSK) (Fig. 1) (Wang et al. 2002). The surface rivers are usually dry. The Qingshan Reservoir only receives surface water from the Dengzhan and Haoying rivers during flood periods. The reservoir outflow discharges into the Houzhai River, part of it entering the DYZ-MSK subterranean river and flowing westward to the watershed outlet at Houzhai (HZ) station. The exposed subterranean river reaches are located at Laoheitan (LHT), Liugu (LG), and Maoshuikeng (MSK), where three hydrological observation stations were set to record groundwater discharge.

Methods

Numerical modeling methods

The code MODFLOW-2005 (Harbaugh 2005) was used to simulate groundwater flow and to evaluate recharge and discharge. In modeling, the study area was discretized into 96 by 124 horizontal grid points in one layer. The total grid space is 100 m. The computational time step is 1 day.

Hydrological boundaries of surface and subterranean watersheds are mostly overlapped. Boundaries in the north and southwest are divided by a topographic boundary and the bedrock consists of mostly less permeable shale and marlite. The east and southeast boundaries are controlled by the Yuguan fault, which acts as a no-flow boundary. The southwest boundary has a flow exchange with the Mugong River but the exchange rate is much smaller and can be neglected. Underground flow from the Maoshuikeng (MSK) outlet is controlled by a fault located near the west topography boundary. The aquifer bedrock is shale and marlite.

There are no regular groundwater observation wells in the study watershed. An initial groundwater level was estimated roughly on the basis of stream levels at 10 stations during the drought period of 1988 and groundwater table slopes investigated by Yu et al. (1990) (Fig. 1). The estimated groundwater table was used as the input of a steady state flow model. The model's output of spatial distribution of a groundwater table was taken as an initial condition for the transient-state flow model. The groundwater evapotranspiration loss was neglected because the depth to groundwater was greater than 3 m in most areas and could reach over 10 m in the upper areas of the study watershed.

The aquifer is regarded as porous Darcy flow and so the River package and Drain package are applied to simulate water exchange between subsurface rivers and the aquifer and between surface rivers and the aquifer, respectively. A large value, around 20,000 m^2/day, was set for the hydraulic conductance of surface river and subterranean

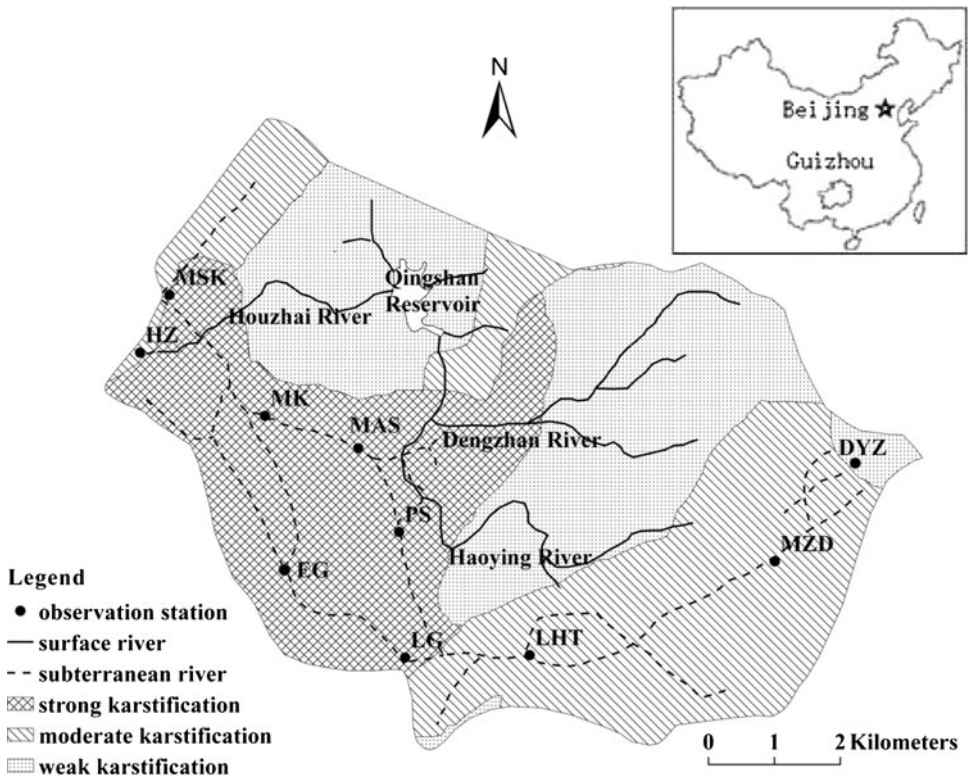

Fig. 1 Houzhai karst system and stream network

river deposits because of a close hydraulic connection between groundwater and river flows through rich rock fractures.

Determination of hydrogeological parameters

Precipitation is a primary source of groundwater recharge. Precipitation recharge is estimated as a daily amount by multiplying the precipitation by a precipitation coefficient (C_{pr}), which is defined as the ratio of multi-year, averaged groundwater recharge to annual average precipitation. For most precipitation events, the recharge amount is approximately equal to underground outflow from the recharge zone. Since precipitation recharge depends on soil, topography, and land surface cover, the study watershed was divided into three sub-regions. The sub-region coefficients were calibrated against observed water levels of subterranean rivers at three sites in 1988 and 1989.

The first sub-region, with an area of 25.4 km^2, is located in the upper region of the study basin from the west boundary to LHT station, consisting of naked karst peak clusters with many depressions (Wang et al. 2002). The soil is thin, less than 50 cm thick. Many ponors, or funnels, which are directly linked with the subterranean rivers, result in a sharp rise and drop of the hydrograph at MZD and LHT stations (Fig. 1). The second sub-region, with an area of 22.7 km^2, is located in the southwest area at LG, EG, PS and MK stations where the watershed drainage reaches the peak forest basin with isolated cones and broad and flat peneplains (Fig. 1). The sub-region is soil covered. The dendritic surface drainage and subterranean water systems overlap or become cross-connected. The enhanced regulating ability of the river system and soil leads to a relatively smooth hydrograph at the monitoring stations. The third sub-region, with an area of 32.8 km^2, is located in the northwest region of Haoying, Dengzhan, and Houzhai rivers, where the landform is relatively flat; depth to groundwater is relatively shallow and soil is thick.

Hydraulic conductivity (K) was initially estimated by analyzing recession hydrographs of stream flow discharges at LHT and MSK stations using Brutsaert and Lopez (1998) and Mendoza et al. (2003) methods. The estimated hydraulic conductivities range between 10^{-5} and 10^{-3} m/s (Freeze and Cherry 1979). For describing properties of the in homogenous and anisotropic aquifer controlled by fractures (Fig. 2), the basin was divided into nine subareas with different horizontal hydraulic conductivity values (K_x in Table 1) and horizontal anisotropy (the ratio of hydraulic conductivities, K_y and K_x, in orthogonal, horizontal directions) according to degree of karstified aquifer (Fig. 1) and dominant fracture directions (Fig. 2). In general, direction of hydraulic conductivity is parallel to the dominant tectonic lines in northeast and north-northeast. Specific yield is set at a value of 0.05 in this study (Gouisset 1981; Smart and Friederich 1986).

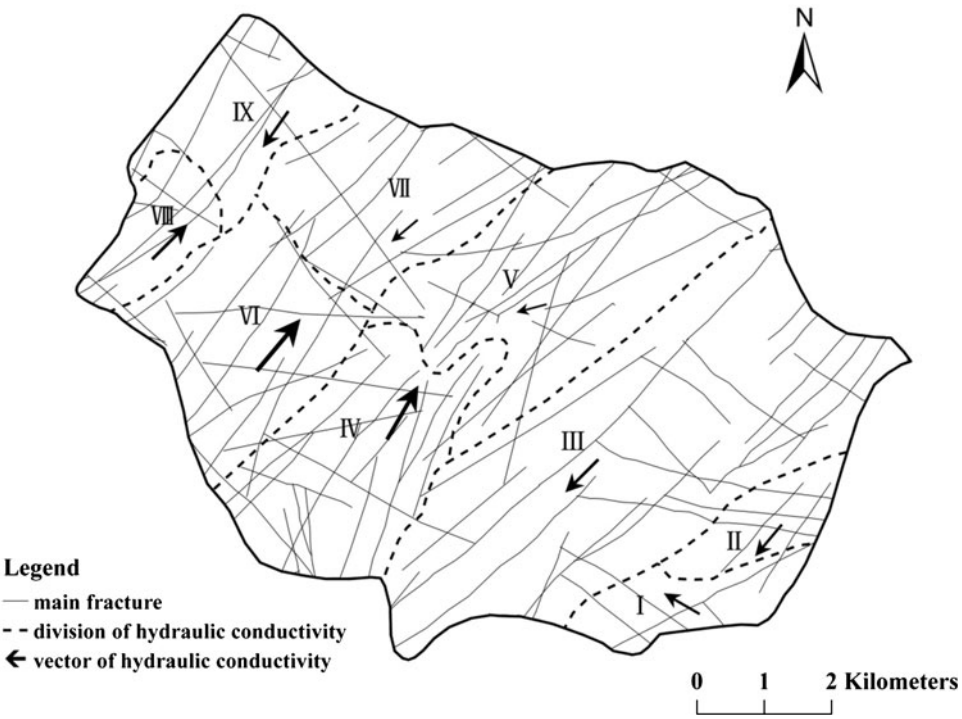

Fig. 2 Main fractures and division of hydraulic conductivity

Table 1 Hydraulic conductivity and precipitation coefficient in the study basin

Sub-areas	I	II	III	IV	V	VI	VII	VIII	IX
K_x (m/day)	6.53	6.53	10.8	17.56	2.47	20.6	2.53	12.2	8.2
HANI	0.58	1.19	1	1.73	0.47	1.19	0.84	1	1.43
C_{pr}	0.473			0.503	0.483	0.503	0.483		

Results

The model parameters were calibrated using a trial and error method. The precipitation coefficients were 0.47, 0.50, and 0.49 in the east, southwest, and west regions (C_{pr} in Table 1), respectively, on the basis of simulated and observed amount of underground flow discharge during 1988 and 1989 at LHT, LG and MSK, respectively. It means that about 48.6 % of precipitation recharges into the aquifer for the basin average. Generally, there are no significant differences for the precipitation coefficient values in the three sub-regions. The coefficient is 0.503 in the southwest sub-region with rich subterranean rivers, a little larger than values in other two sub-regions. Hydraulic conductivities were generally low in the weak karstification area (2.47–8.20 m/day) (Table 1). A low value of hydraulic conductivity (6.53 m/day) was also assigned to the east mountainous areas (I and II in Fig. 2). Much higher hydraulic conductivities (20.6 m/day) were in the area of more intense karst development which has rich subterranean rivers since the confluence of conduit flow increases dissolution in the areas. Anisotropy of hydraulic conductivity reflects regional groundwater flow directions controlled by primary fractures in the directions of northeast and north-northeast. Resulting horizontal anisotropy (HANI) values are larger than 1.0 in most sub-areas (Table 1).

Sensitivity analysis demonstrates that hydraulic conductivity is more sensitive to water table than specific yield. A 50 % decrease of hydraulic conductivity would result in over 0.8 m increase of water tables at MSK and LHT stations, while a 50 % decrease of specific yield would result in less than 0.3 m increase of water tables. Generally, both parameters are insensitive to water table at LG station. A 50 % change in hydraulic conductivity and specific yield results in less than 0.1 m change of water table at LG station.

Comparison of simulated and observed water levels (SWT and OWT in Fig. 3) at three observation stations yields mean absolute errors (MAE) and root mean square errors (RMSE) that are less than 0.126 m (Table 2) during the calibration and validation periods, which represent about 10 % of the water table variations. The correlation coefficients (C_{eff}) between simulated and observed water

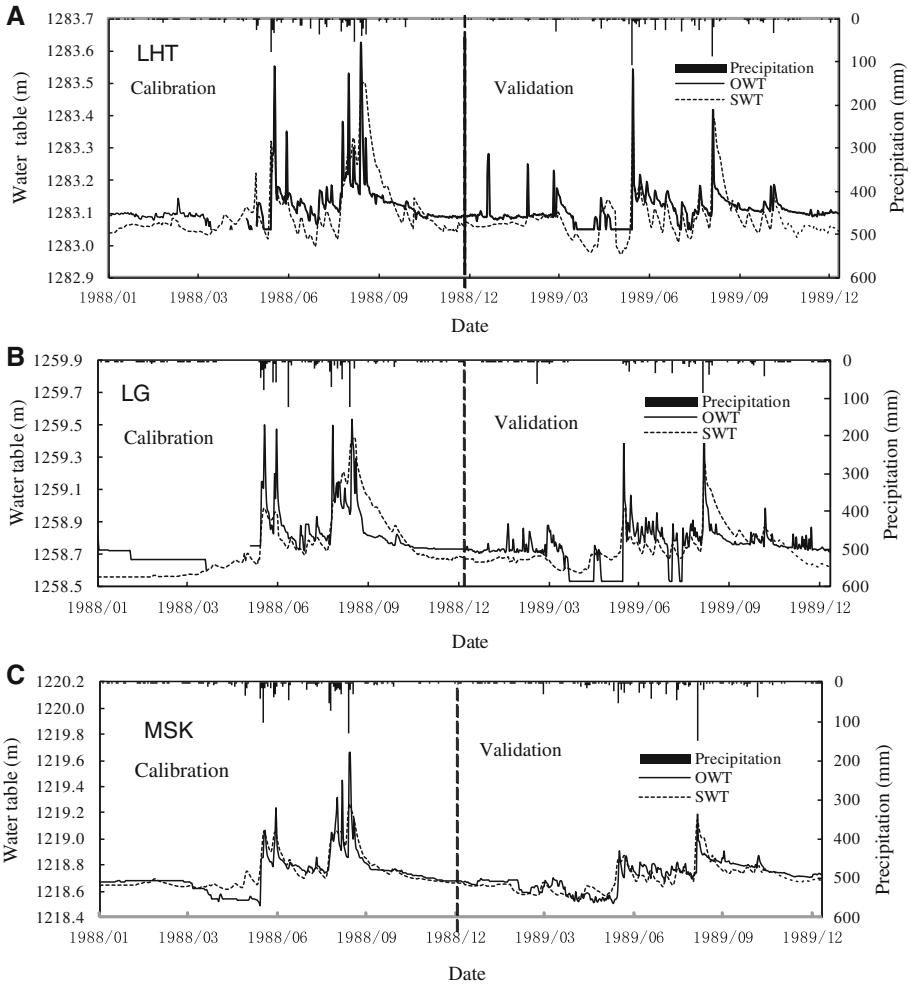

Fig. 3 Simulated and observed water tables during 1988 ~ 1989

Table 2 Statistical results of mean absolute error (MAE), root mean square error (RMSE) and correlation coefficient (C_{eff}) between simulated and observed water tables during calibration period (1988) and validation period (1989)

Station	Calibration period			Validation period		
	MAE (m)	RMSE (m)	C_{eff}	MAE (m)	RMSE (m)	C_{eff}
LHT	0.052	0.070	0.71	0.046	0.056	0.64
LG	0.101	0.104	0.80	0.084	0.126	0.61
MSK	0.051	0.078	0.86	0.05	0.063	0.82

tables (Table 2) indicate generally good agreement between observed and simulated water tables at three stations. Slopes of the simulated recessions at LHT and LG stations are more gradual than the observed recessions because of the forested peak and valley landforms and the great variation of hills and depressions. The transient runoff is not taken into consideration in the recession simulation.

The simulated water balance in the aquifer demonstrates that the total aquifer recharge mostly comes from precipitation and river leakage. Precipitation recharge and river leakage are about 70 and 12 % of the total aquifer recharge, respectively. Meanwhile, large amount of ground flow discharge in the study watershed is from subterranean rivers, which accounts for 62 % of the total discharge. Surface rivers drain only 8 % of the total groundwater discharge which occurs during large flooding periods. During flood periods, decline of surface river levels is faster than that of groundwater levels near the river banks; the hydraulic gradient from the aquifer to the surface river increases and thus groundwater flows into surface rivers.

Conclusions

Procedures for developing the numerical model of the karst basin without detailed groundwater level observations are summarized as: (1) initial groundwater level distribution was simulated using a steady-state flow model with input

of water level observations where groundwater intersects surface features (water tables along rivers and sinkholes) during a drought period. (2) Parameterization of the model was performed on the basis of available water level observations and parameter division based on landforms and geological conditions. Precipitation recharge was estimated by multiplying the daily precipitation by a coefficient. The precipitation coefficient was estimated by total subterranean river discharge divided by total precipitation, and its spatial differences were described by dividing the basin into three sub-regions according to soil, topography, and land surface covers. Hydraulic conductivities were estimated initially using flow recession analysis methods. The regional distribution and anisotropy of hydraulic conductivities were described by the degree of regional karstification and fracture direction. (3) Assessment of the reliability of modeling results depends on calibration and validation of the water levels of subterranean rivers.

The study shows that equivalent porous media models, including exchange of groundwater between surface and subterranean rivers, offered a reasonable description of regional groundwater flow for the karst basin in southwest China. The model generally reproduced temporal variations in water levels with RMSE values of about 10 % of water level fluctuations. It offers estimation of recharge into and discharge from the aquifer which is critical for water resource management and estimation of climate variation influence on river flows.

Acknowledgments This research was supported by National Natural Scientific Foundation of China (No. 40930635, 51079038).

References

Brutsaert W, Lopez JP (1998) Basin-scale geohydrologic drought flow features of riparian aquifers in the southern Great Plains. Water Resour Res 34(2):233–240

Eisenlohr L, Kirtly L, Bouzelboudjen M, Rossier Y (1997) Numerical simulation as a tool for checking the interpretation of karst spring hydrographs. J Hydrol 193:306–315

Freeze RA, Cherry JA (1979) Groundwater. Prentice Hall, Inc., New Jersey

Gouisset Y (1981) Le karst superficiel: genèse, hydrodynamique et caractéristiques hydrauliques. University des Sciences et techniques du Languedoc, Montpellier

Harbaugh AW (2005) MODFLOW-2005, The US geological survey modular ground-water model_the ground-water flow process: US geological survey techniques and methods 6-A16, pp 20–36

Lu Y (2007) Karst water resources and geo-ecology in typical regions of China. Environ Geol 51:695–699

Mendoza GF, Steenhuis TS, Walter MT, Parlangeet JY (2003) Estimating basin-wide hydraulic parameters of a semi-arid mountainous watershed by recession-flow analysis. J Hydrol 279:57–69

Milanovic P (1996) Ombla Spring, Croatia. Environ Geol 27:105–107

Scanlon BR, Mace RE, Barrett ME, Smith B (2003) Can we simulate regional groundwater flow in a karst system using equivalent porous media models? Case study, Barton Springs Edwards aquifer, USA. J Hydrol 276:137–158

Smart PL, Friederich H (1986) Water movement and storage in the unsaturated zone of a maturely karstified carbonate aquifer, Mendip Hills, England. In: Proceedings of the Environmental problems of karst terrains and their solutions conference. National Water Well Association, Dublin, Ohio, pp 59–87

Sun AY, Painter SL, Green RT (2005) Modeling barton springs segment of the edwards aquifer using MODFLOW-DCM. In: Beck BF (ed) Proceedings of the 10th multidisciplinary conference on sinkholes and engineering and environmental impacts of Karst, San Antonio, 24–28 Sept. American Society of Civil Engineers, ASCE Geotechnical Special Publication 144, Reston, pp 163–168

Teutsch G (1993) An extended double-porosity concept as a practical modeling approach for a karstified terrain. In: Günay G, Johnson AI, Back W (eds) Hydrogeological processes in Karst Terranes. Proceedings of the Antalya symposium and field seminar, Antalya, Turkey, 1990: International Association of Hydrological Sciences, Publication No. 207, pp 281–292

Torbarov K (1976) Estimation of permeability and effective porosity in karst on the basis of recession curve analysis. In: Yevjevich V (ed) Karst hydrology and water resources: Proceedings of the U.S.-Yugoslavian Symposium, Dubrovnik, 2–7 June 1975. Water Resources Publications, vol 1, pp 121–136

Wang LC, Zhang JX, Zhou YK, Chen XL, Du JK (2002) Approach of deterministic geomorphologic instantaneous unit hydrograph to hydrological processes' simulation in Karst area. Chin Geogr Sci 12(4):354–358

Wicks CM, Herman JS (1995) The effect of zones of high porosity and permeability on the configuration of the saline freshwater mixing zone. Ground Water 33(5):733–740

Yu JB, Yang LZ, Zhang HS, Fang MZ, Xing FM (1990) Typical study on developmental regularity of karst in China. Science press, China